Towards High Accuracy OCT-based Position Control of a Concentric Tube Robot

K. Rabenorosoa, Y. Baran, G. J. Laurent, P. Rougeot, N. Andreff, and B. Tamadazte

I. Introduction

Concentric tube robots (CTR) are increasingly used in robot assisted interventions [1] due to their compacity, dexterity, and ability to follow complex paths. Several works are focused on the CTR design, modeling, and control [2]–[4]. However, there remain many challenges to make possible realistic and realizable surgical applications [5]. Control of continuum robots is challenging in comparison to that of traditional robots whose links are relatively rigid and whose joints are discrete [5]. In fact, CTR mechanisms are characterized by several specific phenomena like torsion, friction, shear, and non-linear constitutive behaviour. Therefore, ensuring reliable and accurate control of this kind of mechanism is very challenging. One way to control this kind of robot is to use a closed-loop control strategy, for instance, using an image-guided strategy usually called visual servoing control or vision-based control [6]. In fact, image-guided control enables interventional procedures with high accuracy offering very interesting medical outcomes due to the integration of medical imaging system with the surgical work-flow.

The aim of this paper is to perform OCT (optical coherence tomography)-based in-plane positioning task of a CTR system with respect to a biological sample. To do this, we use the B-Scan (2D) OCT images for both the optical biopsy acquisition and the control of the CTR tip. The OCT probe views simultaneously the robot tip and the cross-section of the biological sample. In this work, the CTR is considered such as a puncture needle which must reach, with high accuracy, the optical biopsy site (inside the biological sample). The abstract is organized as follows: Section II presents the used materials and implemented methods while Section III introduces the experimental results.

II. Material and Methods

A. Concentric Tube Robot

A CTR is composed of two main parts: the actuator unit and the backbone as shown in Fig. 2. Note that a CTR system with three tubes is usually proposed to obtain six degrees-of-freedom (DOF) [7], [8]. Usually, the actuator space is defined by $\mathbf{q}=[\alpha_1, \rho_1, \alpha_2, \rho_2, \alpha_3, \rho_3,]^\top$ (Fig. 1) and the robot pose is noticed by ${}^{0}\mathbf{T_3}$. The complete analytic Jacobian matrix of the robot is studied in [8].

All authors are with FEMTO-ST Institute, AS2M department, Univ. Bourgogne Franche-Comté/CNRS, 24 rue Savary, 25000 Besançon, France. kanty.rabenorosoa@femto-st.fr

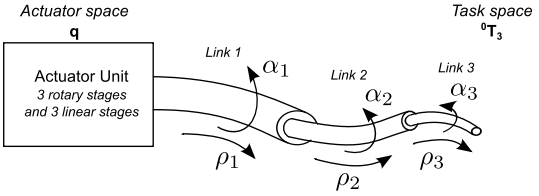

Fig. 1. Working principle of CTR including three curved tubes.

B. OCT Imaging System

The most promising optical biopsy technique is certainly the optical coherence tomography (OCT). OCT is operating under the principle of low coherence interferometry providing very interesting lateral and axial resolutions: 4μm and 3μm, respectively. Since the OCT systems are fiber-optic based principles, it becomes possible to be easily integrated in endoscopic systems for visualizing internal organs. OCT has also been used to perform an ophthalmic surgery [9] and an automatic and repetitive optical biopsy using an OCT-based visual servoing controller [10], [11]. In this work, the used OCT system is a Telesto-II 1300nm marketed by THORLABS.

Probably, the more challenging task in an OCT-based visual servoing process is the ability to extract and track over time visual features, especially when it concerns the visualization of a biological sample. It can be highlighted that OCT images are characterized by a high image noise (e.g., weak signal to noise ratio) and a low texture. Consequently, the visual tracking of the current visual features $\mathbf{s}(t)$ becomes difficult. However, due the fact that this work deals mainly with the control of a CTR mechanism using the OCT images as signal inputs in the control loop, we have chosen to minimize the image processing task. Thus, to tackle this problem of tracking, we implement a conventional normalized cross-correlation (NCC) [12] method to follow over time the robot tip in the OCT images.

C. Experimental Setup

The whole system (Fig. 2) was mounted in an *eye-to-hand* configuration. This means that the OCT imaging system is placed upper the robot tip as well as the biological sample. This configuration allows a simultaneous visualization of the robot tip and the biological sample (Fig. 3). The considered OCT images are B-scan slices (acquired in the xy plane) having a resolution of 500 $\times$ 350 pixels grabbed under a frame-rate up to 25 frames per second.

In practical implementation, the control law processes the

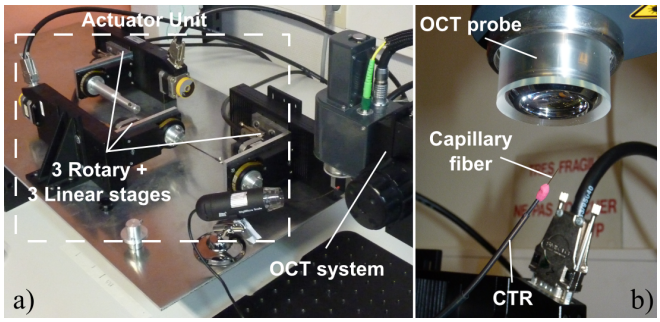

Fig. 2. a) The developed CTR prototype with three curved tubes and the OCT system, b) a zoom on the capillary fiber and the OCT probe positioned in an *eye-to-hand* configuration.

variation of the robot actuator $\delta\mathbf{q}$ in order to reach the fixed tolerance threshold ξ and it is stopped when $\mathbf{e} \leq \xi$.

D. Results

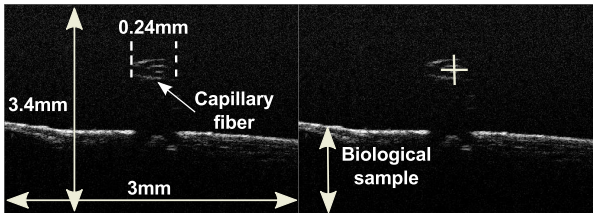

Fig. 3. a) The developed CTR prototype with three curved tubes and the OCT system, b) a zoom on the capillary fiber and the OCT probe positioned in an *eye-to-hand* configuration.

First, 1D positioning tests are performed along X and Y axis in order to validate the proposed control scheme. Then, a 2D control was tested to characterise its performance.

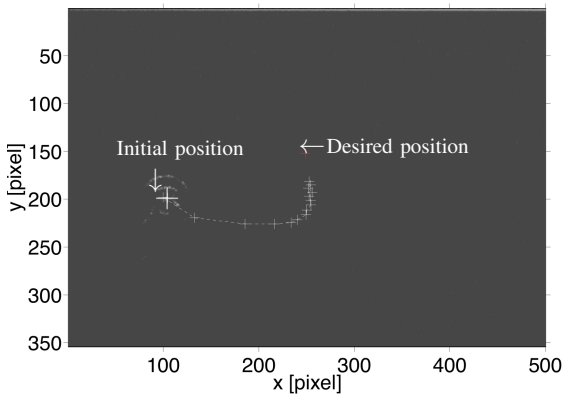

Fig. 4. 2D positioning with λ=0.1, ξ=300 μm, and iteration=19.

The final positioning error is estimated to be 295μm during the test presented in Fig. 4 which can be easily reduced by varying λ and ξ. For instance, a positioning error of 55μm is obtained for λ=0.1 and ξ=100μm. One can observe that the followed trajectory to reach the desired position is not in straight line. This can be explained by the coefficients of the estimated Jacobian matrix where α_3 generates large movements along X and Y compared to ρ_3=ρ_2 ones. In addition, differential kinematics based control of CTR has demonstrated a non-linear behavior in the image plane as reported previously in [6]. This behavior could be explained by the friction and the torsion observed when it concerns large displacements of the tubes.

III. Conclusion

In this abstract, the preliminary results on OCT-based control of CTR are presented which can be considered as original $w.r.t$ to the literature. In fact, the proposed control scheme is experimentally validated in 1D as well as in 2D positioning tasks. It was demonstrated that using OCT system as sensor allows achieving high accuracy positioning task (up to 10μm position error). Future works will be focused on the extension of the proposed control law in order to control more than 2 DOF (e.g., out of plane positioning tasks).

Acknowledgment

This work is conducted with a financial support from the project NEMRO (ANR-14-CE17-0013-01) funded by the ANR and the financial support of the Franche-Comté région (FRANCHIR), France. It is also performed in the framework of the Labex ACTION (ANR-11-LABEX-01-001).

References

[1] J. Burgner-Kahrs, D. C. Rucker, and H. Choset, "Continuum robots for medical applications: A survey," *IEEE Trans. on Robotics*, vol. 31, no. 6, pp. 1261–1280, 2015.

[2] P. E. Dupont, J. Lock, B. Itkowitz, and E. Butler, "Design and control of concentric-tube robots," *IEEE Trans. on Robotics*, vol. 26, pp. 209–225, 2010.

[3] I. R. J. Webster and B. A. Jones, "Design and kinematic modeling of constant curvature continuum robots: A review," *Int. J. of Robotics Research*, vol. 29, pp. 1661–1683, 2010.

[4] C. Girerd, K. Rabenorosoa, and P. Renaud, "Combining tube design and simple kinematic strategy for follow-the-leader deployment of concentric-tube robots," in *Advances in Robot Kinematics*, 2016.

[5] H. B. Gilbert, D. C. Rucker, and R. J. Webster III, "Concentric tube robots: The state of the art and future directions," in *Robotics Research*. Springer, 2016, pp. 253–269.

[6] R. J. Webster III, J. P. Swensen, J. M. Romano, and N. J. Cowan, "Closed-form differential kinematics for concentric-tube continuum robots with application to visual servoing," in *Experimental Robotics*. Springer, 2009, pp. 485–494.

[7] Z. Li, L. Wu, H. Ren, and H. Yu, "Kinematic comparison of surgical tendon-driven manipulators and concentric tube manipulators," *Mechanism and Machine Theory*, vol. 107, pp. 148–165, 2017.

[8] M. T. Chikhaoui, K. Rabenorosoa, and N. Andreff, "Kinematics and performance analysis of a novel concentric tube robotic structure with embedded soft micro-actuation," *Mechanism and Machine Theory*, vol. 104, pp. 234–254, 2016.

[9] H. Yu, J.-H. Shen, K. M. Joos, and N. Simaan, "Calibration and integration of b-mode optical coherence tomography for assistive control in robotic microsurgery," *IEEE/ASME Trans. on Mechatronics*, vol. 21, no. 6, pp. 2613–2623, 2016.

[10] M. Ourak, B. Tamadazte, and N. Andreff, "Partitioned camera-*OCT* based 6 dof visual servoing for automatic repetitive optical biopsies," in *IEEE/RSJ Int. Conf. on Intelligent Robots and Systems*. , Daejean, 2016, pp. 2337–2342.

[11] M. Ourak, A. De Simone, B. Tamadazte, G. J. Laurent, A. Menciassi, and N. Andreff, "Automated in-plane oct-system positioning towards repetitive optical biopsies," 2016 IEEE int. Conf. on Robotics and Automation, Stockholm, 2016, pp. 4186-4191.

[12] D. Forsyth and J. Ponce, Eds., *Computer Vision A Modern Approach*. Pearson, 2012.